RESEARCH ARTICLE

The development of brain functional connectivity networks revealed by resting-state functional magnetic resonance imaging

Chao-Lin Li[1, 6, *], **Yan-Jun Deng**[2], **Yu-Hui He**[3], **Hong-Chang Zhai**[4], **Fu-Cang Jia**[5]

1 School of Education, South China Normal University, Guangzhou, Guangdong Province, China
2 School of Psychology, South China Normal University, Guangzhou, Guangdong Province, China
3 Donghui Kindergarten, Huangpu District, Guangzhou, Guangdong Province, China
4 School of Education, Guangzhou University, Guangzhou, Guangdong Province, China
5 Research Lab for Medical Imaging and Digital Surgery, Shenzhen Institutes of Advanced Technology, Chinese Academy of Sciences, Shenzhen, Guangdong Province, China
6 Center of Network and Modern Educational Technology, Guangzhou University, Guangzhou, Guangdong Province, China

Funding: *This study was supported by the Natural Science Foundation of Guangdong Province, No. 2016A030313180 (to FCJ).*

Graphical Abstract

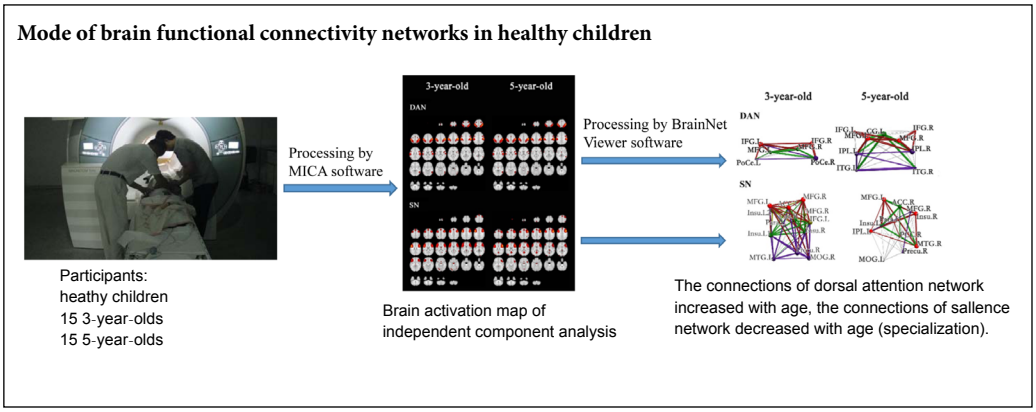

Correspondence to:
Chao-Lin Li,
lichaolin@m.scnu.edu.cn.

orcid:
0000-0002-7438-6706
(Chao-Lin Li)

doi: *10.4103/1673-5374.253526*

Received: *October 9, 2018*
Accepted: *February 14, 2019*

Abstract

Previous studies on brain functional connectivity networks in children have mainly focused on changes in function in specific brain regions, as opposed to whole brain connectivity in healthy children. By analyzing the independent components of activation and network connectivity between brain regions, we examined brain activity status and development trends in children aged 3 and 5 years. These data could provide a reference for brain function rehabilitation in children with illness or abnormal function. We acquired functional magnetic resonance images from 15 3-year-old children and 15 5-year-old children under natural sleep conditions. The participants were recruited from five kindergartens in the Nanshan District of Shenzhen City, China. The parents of the participants signed an informed consent form with the premise that they had been fully informed regarding the experimental protocol. We used masked independent component analysis and BrainNet Viewer software to explore the independent components of the brain and correlation connections between brain regions. We identified seven independent components in the two groups of children, including the executive control network, the dorsal attention network, the default mode network, the left frontoparietal network, the right frontoparietal network, the salience network, and the motor network. In the default mode network, the posterior cingulate cortex, medial frontal gyrus, and inferior parietal lobule were activated in both 3- and 5-year-old children, supporting the "three-brain region theory" of the default mode network. In the frontoparietal network, the frontal and parietal gyri were activated in the two groups of children, and functional connectivity was strengthened in 5-year-olds compared with 3-year-olds, although the nodes and network connections were not yet mature. The high-correlation network connections in the default mode networks and dorsal attention networks had been significantly strengthened in 5-year-olds *vs.* 3-year-olds. Further, the salience network in the 3-year-old children included an activated insula/inferior frontal gyrus-anterior cingulate cortex network circuit and an activated thalamus-parahippocampal-posterior cingulate cortex-subcortical regions network circuit. By the age of 5 years, nodes and high-correlation network connections (edges) were reduced in the salience network. Overall, activation of the dorsal attention network, default mode network, left frontoparietal network, and right frontoparietal network increased (the volume of activation increased, the signals strengthened, and the high-correlation connections increased and strengthened) in 5-year-olds compared with 3-year-olds, but activation in some brain nodes weakened or disappeared in the salience network, and the network connections (edges) were reduced. Between the ages of 3 and 5 years, we observed a tendency for function in some brain regions to be strengthened and for the generalization of activation to be reduced, indicating that specialization begins to develop at this time. The study protocol was approved by the local ethics committee of the Shenzhen Institute of Advanced Technology, Chinese Academy of Sciences in China with approval No. SIAT-IRB-131115-H0075 on November 15, 2013.

Key Words: *nerve regeneration; functional MRI; brain network; functional connectivity; resting-state; ICA; brain development; children; resting-state networks; infant template; standardized; neural regeneration*

Chinese Library Classification No. *R445; R725*

Introduction

Previous studies of brain network abnormalities in children have mainly focused on one network, such that few studies examined the whole brain network. For example, one study examined the default mode network, central executive network, core network, visual network, and self-referential network in individuals with autism spectrum disorder (Bi et al., 2018), while another discussed executive control, cerebellar and frontoparietal networks, and default-mode networks in those with attention-deficit/hyperactivity disorder (Mostert et al., 2016). Comprehensive surveys are necessary to fully characterize changes in brain networks, including those associated with development and illness/injury. In terms of comparative studies in which patients and normal children were assessed, more studies have examined individual brain networks compared with whole brain networks. With respect to comparative statistical analyses of patients and healthy controls, some studies used independent component analysis (ICA) to compare two groups (Gao et al., 2009) while others examined group differences. Relevance or regression analyses have been used to identify intergroup differences among six brain networks in patients with attention-deficit/hyperactivity disorder (Gao et al., 2009; Nomi and Uddin, 2015). Statistical analyses in brain network research can be complex compared with analyses generally used in behavioral experimental research, as brain networks contain many factors, such as edges, nodes, cores, and correlation coefficients between brain regions. Although many methods are available for conducting statistical comparisons of the intensity of brain networks, few studies have produced detailed descriptions of the specific brain regions within a network.

Measurement of blood oxygen level-dependent signals using functional magnetic resonance imaging (fMRI) has become a strong tool for probing neural development in the human brain. Since Biswal et al. (1995) reported that different brain regions show synchronous fluctuations of intrinsic activity, researchers have attempted to examine these spontaneous low-frequency (< 0.1 Hz) patterns. Recently, ICA has been successfully applied to the estimation of some low-frequency modes (Deng et al., 2016; Lin et al., 2017). Compared with hypothesis-based techniques, this exploratory technique is advantageous in that it can use spatial and/or temporal characteristics to identify various types of signal fluctuations without specifying an explicit temporal model.

Doria et al. (2010) found that between 29 and 43 weeks of age, executive control, frontoparietal networks, and default mode networks develop at different rates. In 5- to 8-year-old children, most resting-state networks have developed, but the default mode network is immature, with incomplete and fragmented patterns of functional connectivity (de Bie et al., 2012). As an individual develops, the default network grows until it resembles that of adults, and includes the posterior cingulate cortex/retrosplenial (PCC/Rsp), lateral temporal cortex, inferior parietal lobule, regions of the hippocampus, and the medial prefrontal cortex (Gao et al., 2009). In children, the major nodes of the default network appear at 3–5 years (Xiao et al., 2016) and 7–9 years (Fair et al., 2008) of age, although the network connections are not mature at these time points.

Although previous studies have examined brain function development in preschool children in the resting state, few studies have conducted systematic examinations of the development of independent components of brain function.

The experimental subjects in the above studies were primarily children under 2 years of age. Indeed, few resting-state fMRI experiments have examined children ages 3 and 6. ICA is frequently used to examine independence from prior hypotheses (Lee et al., 2013). Studies often examine a single group of children or adults, and studies with intergroup designs focused on preschool children are limited. Few systematic investigations have examined preschool children of different ages. The mechanisms of brain function in preschool-age children may reveal trends in brain development. As the number of nodes in activated brain areas is affected by statistical parameters (*P* value, threshold, multiple comparison threshold value), it is difficult to obtain consistent results regarding the number of nodes of brain activation. Relatively stable characteristics of the individual components of brain activation areas can be revealed using brain network analysis. In this study, we used a combination of brain network analysis methods to examine the mechanisms governing the development of individual brain network components in children of different ages.

Participants and Methods

Participants

fMRI studies with newborns and children aged 1–2 years are facilitated by the large amount of time that these children spend sleeping (Konishi et al., 2002; Grossmann et al., 2007), and thus, resting-state research has been conducted in these age groups. Similarly, by the age of 6 or 7 years, children can cooperate to complete experimental tasks (Gomot et al., 2006). However, children aged 3–5 years may not have sufficient concentration or comprehension to undergo MRI examination in an awake state, and thus experiments with this age group are rarely reported. However, the age of 3–5 years represents the period in which language develops most quickly. Penfield, Roberts, and later Lenneberg suggested that this was the "critical period" for child development (Penfield and Roberts, 1959; Lenneberg, 1967). Thus, we chose 3- and 5-year-olds as research subjects.

Recruitments

We recruited participants from five kindergartens in the Nanshan District of Shenzhen City, China. The teachers and parents were informed that participation was voluntary. We introduced the MRI process to the parents and kindergarten teachers of the children, and discussed important points to consider regarding the experience of being inside the machine and possible situations that may arise. Parents were advised to take their children to the hospital for examination if the MRI revealed that the children had suffered a head impact, illness, or had visible brain abnormalities. There

were 36 preschool children in total, including 17 3-year-olds (9 boys, 36 ± 2 months) and 19 5-year-olds (10 boys, 60 ± 2 months).

Inclusion criteria

We enrolled children who were healthy, right-handed, and had normal language development. Before MRI scanning, all subjects were examined using the China-Binet intelligence test, and all scored between 90 and 110 (3-year-olds: 94.00 ± 2.62; 5-year-olds: 97.40 ± 6.48). Children with scores above 90 were included in the trial.

Exclusion criteria

Children with autism, hyperactivity disorder, depression, abnormal language expression, and those who did not have a full-term birth were excluded from participation in the trial.

Withdrawal criteria

Children with scores below 90 in the China-Binet intelligence test were withdrawn from participation in the trial.

Ethics

The study protocol was approved by the local ethical committee at the Shenzhen Institute of Advanced Technology, Chinese Academy of Sciences (No. SIAT-IRB-131115-H0075) on November 15, 2013 (**Additional file 1**). All parents of the children enrolled provided written informed consent (**Additional file 2**).

Methods

fMRI

fMRI scans were performed while the children were asleep. The sessions were 8 minutes long, ensuring that 200 sequences were collected (Gao et al., 2009; Raichle et al., 2001). The TR time was 2.5 seconds. In resting-state studies, data are not expected to vary according to the time of day of data collection. To facilitate sleep in the children in the present study, we conducted scanning from 14:00 to 18:00.

The times required to complete all sequences in the resting state were as follows: 1 minute for positioning the image, 8 minutes for collecting the functional images, and 2 minutes for flash 3D scanning, for a total of 11 minutes. Children were positioned in the MRI scanner and while they were asleep. Each child remained in the scanner for about 20 minutes, such that the total length of the session was 30–40 minutes.

Kindergarten children generally take afternoon naps. After lunch at the kindergarten, the children were sent to the yard near the MRI room instead of taking a nap with the other children in the kindergarten. Teachers and the parents watched and played with the children. This made the children tired, and they slept very easily in the MRI scanner. One hour before the MRI session, a child who was fatigued and thus likely to sleep during scanning was brought to the experimental preparation room and encouraged to fall asleep. After the child had fallen asleep, the parent or kindergarten teacher moved the child to the bed of the MRI scanner while patting them gently and coaxing them to continue to sleep. After the child was asleep, the teacher raised his/her hand to signal the engineer to start scanning. If the child awoke, the parent or teacher continued to coax the child to sleep. If the child did not continue to sleep or woke up during the scanning process, MRI scanning was terminated. Children aged 3 and 5 years cannot maintain a sufficiently motionless position to complete MRI scanning in an awake state. Only sleeping children in this age group can complete the whole scan sequence. We observed involuntary trembling lips or head twisting in two 3-year-olds and one 5-year-old. One 5-year-old coughed during the scanning, and two 5-year-olds exhibited obvious head movements. These children were rescanned after the teacher or parent had coaxed them into a calm sleeping state. At the end of the study, MRI data from 30 children were available, with 15 in each age group. The 3-year-old group (36 ± 2 months) contained seven boys and eight girls, and the 5-year-old group (60 ± 2 months) contained seven boys and eight girls. After preprocessing and assessment of temporal data associated with head movement, the maximum head movement was confirmed to be less than 0.3 mm. Statistical analyses were conducted in these 30 children.

Data acquisition

The MRI scans were conducted in the MRI chamber at the Shenzhen Institute of Advanced Technology, Chinese Academy of Sciences, in March 2015. MRI scans were acquired using a 3.0T MRI scanner (Siemens Magnetom Trio A Tim System) with a 12-channel head coil. The T1 scanning parameters were: echo time (TE) = 9.1, repetition time (TR) = 564 ms, slice thickness = 2.5, gap = 0.5, flip angle = 70°, slice number = 36, field of view (FOV) = 200 × 200, and matrix = 250 × 250. For functional images, we used a $T2^*$-weighted gradient echo sequence with TR = 2500 ms, TE = 30 ms, flip angle = 90°, gap = 0.5, slice thickness = 2.5, FOV = 200 × 200, and matrix = 64 × 64. The whole brain was scanned in 36 slices with 192 volumes, and the collection time adopted the time series commonly used in the resting state. High-resolution three-dimensional structural images were acquired using a T1-weighted, magnetization-prepared rapid gradient echo sequence (TR/TE = 1900.00 ms/2.53 ms, flip angle = 9°, slice thickness = 1.0, gap = 0, FOV = 250 × 250, and matrix = 250 × 250).

Data processing

We used statistical parameter mapping for functional image preprocessing (SPM8, http://www.fil.ion.ucl.ac.uk/spm). To generate magnetization equilibrium, the first 10 volumes of each function time series were discarded. The remaining 180 images were corrected for differences associated with image acquisition time between slices. Head motion was corrected as follows: (1) each time series was despiked to remove extreme outliers; (2) motion of translation larger than 0.2 mm in any direction (X, Y, Z) was censored; (3) a least-squares approach and a 6-parameter (rigid body) spatial transform were used to correct errors associated with head motion

and drifting. Adult templates cannot be used for children. Thus, we used averaged child templates obtained from standardized experimental data as the standardized template for children in this trial. All child data were spatially normalized to the infant template (TLRC space, Cincinnati Children's Hospital Medical Center: https://irc.cchmc.org/software/tom.php), and each voxel was resampled to 3 mm × 3 mm × 3 mm cubic voxels. Average values were calculated respectively for 3-year-olds and 5-year-olds, and two mean child templates were made using the normalized 3D images from the 30 children. Then, the average template was used to standardize the data for each child, and these data were reprocessed based on the mean templates. We used a Gaussian kernel that was 8 mm full width at half-maximum to smooth the data. We used the Resting State fMRI Data Analysis Toolkit (http://www.restfmri.net) for further processing, including temporal bandpass filtering (0.01–0.08 Hz) to decrease the low-frequency drift.

Seven motion correction measurements (three axial measurements, A-P, R-L, and I-S; and three angle measurements, yaw, pitch, and roll) were used to compare head movements between the groups (3-year-old and 5-year-old children). We used an independent samples *t*-test to examine significant differences in the seven movement parameters between the two groups (A–P: $t(28) = 0.019$, $P > 0.05$; R–L: $t(28) = 0.000$, $P > 0.05$; I–S: $t(28) = 0.000$, $P > 0.05$; Yaw: $t(28) = 0.000$, $P > 0.05$; Pitch: $t(28) = 0.000$, $P > 0.05$; Roll: $t(28) = 0.000$, $P > 0.05$). Both groups had a maximum displacement of less than 1 mm in the *X*, *Y*, or *Z*, directions, and we found no significant difference in maximum displacement.

Post-processing and data analysis

We used principal component analysis to reduce the dimensionality of the data, and then performed ICA to obtain a series of aggregate independent components for all age groups. ICA was carried out in each group using the masked ICA (MICA) software (Zhang et al., 2010; Moher Alsady et al., 2016; http://www.nitrc.org/projects/cogicat). In the setup for the ICA, we used the child mean template to represent the child data and a default template to reduce any further scatter. The components generated by the ICA were then clustered to remove outliers. The distance threshold for outlier removal was set at 0.7. Data reduction (principal component analysis) was divided into three steps. We used the default ICA parameters. The ICA was developed so that subjects were grouped in a random order rather than according to the order of the files. Initialization was also randomized, and the number of runs was set to 100. The number of components was set to 30, and the scale of the result was set to "Z-score". We employed three methods to ensure that the components were correct. First, we used activated ICA components from previous studies as references (Jafri et al., 2008; Zhang et al., 2010; Muetzel et al., 2016). Second, we used the ICA template mask (Thomason et al., 2011; http://www.brainnexus.com/resources/resting-state-fmri-templates) as a reference. Third, we used the cluster result generated by AFNI (Cox, 2012). We expected activation to be greater in ICA-named brain areas or ICA-representative brain areas and to be listed at the beginning of the cluster table. For instance, the default mode network was indicated by the PCC, the frontoparietal network by the frontal and parietal gyri, the motor network by the medial frontal gyrus (MeFG), the dorsal attention network by the inferior frontal gyrus (IFG) and inferior parietal lobule, and the salience network by the anterior cingulate cortex and anterior insula/IFG.

We extracted seven components from each group, and performed a one-sample *t*-test on the Fisher's *Z*-transformed group average to determine whether the strength of the connections differed from zero, for all connections. Multiple comparisons were corrected by clustering ($P = 0.001$ and threshold = 4.118, voxels in cluster = 22). We used the average child template for analysis.

Although principal component analysis/ICA were performed for all subjects in all age groups, the two-sample t-test result for each component was not sufficient to reflect the network connection level. Thus, we separately extracted the average time course for each region of interest for each subject and constructed a correlation matrix. Before the correlations were computed, the average time course was low-pass filtered at 0.08 Hz and detrended for the time course for each subject. To combine the correlation coefficients among subjects in different age groups, we applied Fisher's *Z*-transform to each subject and calculated the average among all of the subjects. The average correlation matrix for each group was then determined (converted back to the correlation coefficient for analysis).

Results

Quantitative analysis of participants

There were 36 children enrolled in the trial, including 17 3-year-olds and 19 5-year-olds. Since the scanner was not correctly set up at the beginning, the first 3-year-old child did not have enough time to undertake an MRI scan. As a result, 192 sequences were not collected. Another 3-year-old child woke up during scanning. Although he persisted until the entire scan was complete, as the scan was completed in the awake state, the data were not included. Three of the 5-year-olds woke up during scanning, and the parents/teachers were not able to coax them back to sleep. Another 5-year-old had been playing and did not appear to be tired, and thus did not participate in the scanning. The final analysis included 15 3-year-olds and 15 5-year-olds (**Figure 1**).

Analysis of seven independent brain networks in children

We performed ICA using resting-state fMRI data from 30

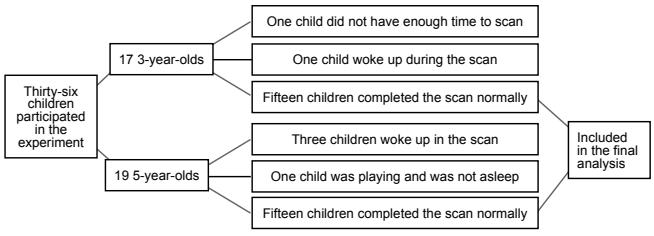

Figure 1 Quantitative analysis of participants.

children (15 at the age of 3 years and 15 at the age of 5 years). We selected and identified several components, including the dorsal attention network, the salience network, the default mode network, the left frontoparietal network, the right frontoparietal network, the executive control network, and the motor network. Spatial maps of the seven selected resting-state networks are shown in **Table 1** and **Figure 2**. The scans were normalized using skull-stripped structural images from Cincinnati Children's Hospital Medical Center, and then average templates for the 3- and 5-year-old groups were computed and used within the ICA. Seven components were identified based on the cluster result. A two-sample *t*-test was performed on each of the seven components. The coordinates for the peak activations in each group are shown in **Table 2**. Resting-state networks were grouped by age.

The number of brain activation areas was affected by the clustering parameters. It was difficult to establish clustering parameters that produced a consistent result. In active brain areas, locations and network connections that were closely correlated were considered to be representative. We conducted statistical analyses to assess the activated brain areas for each component (**Figure 3**).

Default mode network: As the chart shows, in the default mode network for children aged 3, the MeFG.L (left MeFG), PCC, and inferior parietal lobule (IPL) were the most strongly activated regions. These areas represent the most basic brain regions in the early default network. The MeFG-PCC connection had a correlation greater than 0.7. By the age of 5 years, the MeFG-IPL connection also had a correlation greater than 0.7.

Dorsal attention network: Although activation in the IFG and middle frontal gyrus (MFG) was strong in 3-year-old children, it was mainly confined to the frontal region. By the age of 5 years, in addition to the frontal lobe, the IPL and inferior temporal gyrus (ITG) were also strongly activated, and showed an increase in high-correlation connections in the brain. In terms of brain regions with correlations greater than 0.7, 3-year-old children had IFG.L-IFG.R (left-right brain connection) and IFG-MFG (frontal area connection) connections. In 5-year-old children, we found IFG.R-IPL.R and IPL.L-ITG.L (connections among brain regions) connections. We also found a developmental phenomenon where, rather than an increase in the number of activation areas alone, the activation of brain areas and high-correlation connections were altered. For example, while the correlation of the IFG.L-IFG.R connection was more than 0.7 at the age of 3 years, this connection was not very strong at the age of 5 years. We found strong connections in 3-year-old children, such as the IFG.L-MFG.L. While 5-year-old children still had strong connections, activation appeared to both increase and change during development.

Executive control network: The SPL.L was the mostly strongly activated brain area in 3-year-old children, and only SPL.L-Prcu.L and SPL.L-IFG.L were highly correlated, indicating that the frontal area did not play a significant role in controlling the network.

By the age of 5 years, we observed high-correlation connections including IFG.L-IFG.R and IFG.R-MTG.L, which demonstrate that the left-right brain connection and connections among different brain regions were developing and strengthening. However, from a brain network perspective, the weak self-control ability of 3-year-old children is related to brain development.

Frontoparietal network: The frontoparietal network was the best-developed network associated with brain connectivity in 3-year-olds. The connections with correlations higher than 0.7 were SFG.L-IPL.L and SFP.L-Caud.R (MTG.R). The highly correlated network in the left cerebral area in 5-year-olds was greatly enhanced, particularly the MFG.L-SFG.L (IPL.L) and MTG.L-IPL.L connections. Three year olds exhibited imbalanced development on both sides of the brain, indicating that left dominance had not yet been formed. With the development of the network in the right hemisphere, there were more high correlation connections in 5-year-old children.

Salience network: This area of the brain network is mainly located in the IFG. At the age of 3 years, we found more activated areas and high correlation connections. At the age of 5 years, the correlation had decreased. This type of change may be related to specialization of the network and improved efficiency.

Effects of ICA-derived outcome variables

To ensure the representativeness of the extracted components, we examined the effects of ICA-derived outcome variables including the two-dimensional distribution of components (scaled points using multidimensional scaling and raw data scatter) and the stable curves of each component (components were ranked by mean ± SD).

The coordinates of the activated brain areas were clustered into one table. The preprocessed image data showed that the data for the 15 3-year-olds and 15 5-year-olds were jointly accepted in the ICA statistical processing. Seven independent components were extracted. Then, the components were divided into a 3 year old group and a 5 year old group, and a t-test was performed for each group individually. The cluster table was used to ensure that the components were consistent across the two groups (**Table 2**). We obtained an ICA activation map for the preprocessed 3-year-old and 5-year-old groups (**Figure 2**). ICA networks that have been seldom examined, such as the executive control network, salience network, and dorsal attention network, may be used as references for the ICA results.

Default mode network: A number of brain areas, including the precuneus, left/right inferior parietal lobules, posterior cingulate, medial frontal gyrus, and MTG are known to be activated *via* resting-state network connections in adults. In the two groups of children in the present study, only the posterior cingulate, inferior parietal lobule, and medial

Table 1 Clustered areas of significant activation according to independent component analysis

	3-year-olds				5-year-olds			
	Brain region	Abbr	Vol (mm^3)	MNI (*X*, *Y*, *Z*, mm)	Brain region	Abbr	Vol (mm^3)	MNI (*X*, *Y*, *Z*, mm)
D	R Posterior Cingulate (BA30)	PCC	2877	6, –54, 18	R Posterior Cingulate (BA23)	PCC	2728	6, –48, 24
M	L Inferior Parietal Lobule (BA39)	IPL	190	–44, –70, 38	L Medial Frontal Gyrus (BA32)	MeFG	169	–2, 50, –2
N	R Middle Occipital Gyrus	MOG	184	34, –90, –4	L Inferior Parietal Lobule (BA39)	IPL	90	–42, –66, 40
	L Medial Frontal Gyrus (BA10)	MeFG	128	–4, 50, –4	R Middle Frontal Gyrus	MFG	36	34, 14, 42
D	L Postcentral Gyrus (BA3)	PoCe	1703	–60, –24, 44	R Inferior Parietal Lobule (BA40)	IPL	1520	52, –30, 48
A	R Postcentral Gyrus (BA2)	PoCe	1691	60, –22, 30	L Inferior Parietal Lobule (BA40)	IPL	1362	–50, –34, 48
N	R Inferior Frontal Gyrus (BA44)	IFG	189	52, 8, 24	R Inferior Frontal Gyrus (BA9)	IFG	123	58, 8, 26
	R Middle Frontal Gyrus (BA6)	MFG	58	24, –4, 62	L Inferior Frontal Gyrus (BA9)	IFG	90	–54, 6, 36
	L Middle Frontal Gyrus (BA6)	MFG	48	–30, –10, 62	L Inferior Temporal Gyrus	ITG	58	–50, –64, –6
	L Inferior Frontal Gyrus (BA9)	IFG	31	–50, 6, 32	R Middle Frontal Gyrus (BA6)	MFG	54	28, –10, 66
					L Middle Frontal Gyrus (BA6)	MFG	41	–30, –6, 62
					L Cingulate Gyrus	CG	38	–0, 2, 36
					R Inferior Temporal Gyrus	ITG	30	58, –60, –12
E	L Inferior Frontal Gyrus (BA46)	IFG	2506	–42, 42, 12	L Inferior Frontal Gyrus (BA45)	IFG	2798	–50, 26, 8
C	R Inferior Frontal Gyrus	IFG	1024	48, 44, 0	R Inferior Frontal Gyrus	IFG	776	48, 32, 6
N	L Superior Parietal Lobule (BA7)	SPL	329	–32, –60, 50	L Precuneus (BA39)	Prcu	390	–30, –66, 36
	R Middle Occipital Gyrus (BA18)	MOG	142	30, –96, –6	R Cuneus (BA18)	Cun	112	28, –100, –6
	L Precuneus (BA31)	Prcu	38	–8, –72, 18	L Middle Temporal Gyrus (BA21)	MTG	80	–62, –40, –10
					R Inferior Temporal Gyrus (BA37)	ITG	56	60, –58, –10
L	L Inferior Parietal Lobule (BA39)	IPL	2437	–42, –72, 38	L Inferior Parietal Lobule	IPL1	2266	–48, –48, 28
F	L Superior Frontal Gyrus (BA9)	SFG	263	–24, 42, 38	L Superior Frontal Gyrus (BA6)	SFG	420	–18, 26, 60
P	L Middle Temporal Gyrus (BA21)	MTG	252	–56, –16, –18	L Middle Temporal Gyrus	MTG	96	–50, –28, –10
	L Culmen	Culm	116	–6, –70, –16	L Middle Frontal Gyrus	MFG	56	–36, 26, 48
	R Middle Temporal Gyrus	MTG	52	34, –58, 20	L Inferior Parietal Lobule	IPL2	30	–32, –28, 30
	R Caudate	Caud	38	22, –30, 24				
	L Precuneus	Prcu	38	–12, –70, 62				
R	R Inferior Parietal Lobule (BA40)	IPL	1328	46, –66, 44	R Inferior Parietal Lobule (BA40)	IPL	1342	48, –54, 44
F	L Inferior Parietal Lobule (BA40)	IPL	856	–50, –64, 48	L Inferior Parietal Lobule (BA40)	IPL	872	44, –64, 48
P	R Middle Frontal Gyrus (BA9)	MFG	520	40, 30, 38	R Middle Temporal Gyrus (BA21)	MTG	361	60, –24, –6
	R Middle Temporal Gyrus (BA21)	MTG	427	64, –28, –6	R Middle Frontal Gyrus (BA9)	MFG1	267	42, 26, 42
	L Middle Temporal Gyrus (BA21)	MTG	143	–62, –28, –12	R Middle Frontal Gyrus (BA10)	MFG2	257	36, 42, 0
	R Cingulate Gyrus (BA31)	CG	96	4, –30, 38	L Middle Temporal Gyrus (BA21)	MTG	135	–62, –40, –6
	L Middle Frontal Gyrus (BA10)	MFG	93	–38, 54, 0	R Cingulate Gyrus	CG	102	6, –36, 44
					L Inferior Frontal Gyrus (BA10)	IFG	72	–44, 48, 2
					R Precuneus (BA7)	Prcu	61	6, –76, 48
					L Middle Frontal Gyrus (BA8)	MFG	46	–36, 20, 50
					R Inferior Frontal Gyrus (BA45)	IFG	33	54, 18, 6
S	R Middle Frontal Gyrus (BA10)	MFG	1605	30, 42, 24	R Anterior Cingulate	ACC	2882	4, 26, 28
N	L Anterior Cingulate	ACC	780	–0, 26, 28	L Middle Frontal Gyrus (BA10)	MFG	526	–32, 42, 18
	R Insula (BA13)	Insu	426	34, –24, 12	Right Insula (BA13)	Insu	320	40, 10, 18
	L Middle Frontal Gyrus (BA9)	MFG	364	–38, 30, 36	R Posterior Cingulate (BA29)	PCC	189	4, –42, 14
	L Insula (BA13)	Insu	316	–36, –30, 20	Left Insula (BA13)	Insu	112	–38, –18, 18
	L Inferior Frontal Gyrus (BA9)	IFG	98	44, –4, 24	L Inferior Parietal lobule (BA40)	IPL	103	–62, –30, 26
	R Caudate	Cau	90	12, –0, 12	R Precuneus (BA7)	Precu	65	10, –78, 48
	R Precuneus	Precu	85	18, –66, 24	R Middle Frontal Gyrus (BA6)	MFG	58	28, 14, 62
	R Middle Frontal Gyrus (BA6)	MFG	55	34, 12, 62	R Middle Temporal Gyrus (BA39)	MTG	37	42, –64, 18
	L Insula (BA13)	Insu	41	–32, 20, 12	L Parahippocampal Gyrus	Para	35	–8, –10, –18
	L Parahippocampal Gyrus	Para	40	–6, –10, –22	L Middle Occipital Gyrus (BA18)	MOG	26	–32, –96, 6
	R Middle Occipital Gyrus	MOG	36	42, –76, 14				
	L Middle Temporal Gyrus	MTG	36	–30, –78, 20				
M	R Precentral Gyrus (BA6)	PreCe	1291	58, –5, 36	R Precentral Gyrus (BA6)	PreCe	1140	58, –8, 39
O		Ins	1105	–39, –13, 16	L Precentral Gyrus (BA4)	PreCe	956	–58, –17, 38
T	L Insula (BA13)				L Angular Gyrus (BA39)	Ang	36	–42, –70, 35
O								

L: Left; R: right; abbr: abbreviations; Brodmann's areas in "( )", X, Y, and Z: coordinates shown in Montreal Neurological Institute (MNI) space for the peak voxel in each activated region. Vol: voxel size is 3 mm × 3 mm × 3 mm. Anterior cingulate activation overlaps with that in the inferior frontal gyrus (IFG) in the salience network (SN). Activation maps were generated for seven independent brain networks in 3-year-old and 5-year-old children in the resting state. These included the dorsal attention network (DAN), the SN, the default mode network (DMN), the left frontoparietal network (LFP), the right frontoparietal network (RFP), the executive control network (ECN), and the motor network (MOTO).

Table 2 Areas with significant activation by cluster: pairwise two-sample *t*-test analysis (*P* = 0.01)

	Brain region	Vol (mm^3)	MNI (*X*, *Y*, *Z*, mm)
	5-year-olds *vs.* 3-year-olds		
DMN	Left Middle Temporal Gyrus	29	–42, 46, –4
DAN	Right Middle Frontal Gyrus (BA6)	51	36, –12, 48
	Left Precentral Gyrus	39	–24, -22, 66
	Left Middle Frontal Gyrus	30	–42, 6, 50
ECN	Right Superior Temporal Gyrus (BA41)	21	42, –36, 14
	Right Caudate	20	4, 18, 14
LFP	Right Superior Frontal Gyrus	108	10, 26, 48
	Left Precentral Gyrus (BA4)	44	–50, –10, 56
	Left Inferior Parietal Lobule	30	–32, –48, 56
RFP	Left Middle Temporal Gyrus (BA22)	124	–60, –48, 0
SN	Left Middle Temporal Gyrus	44	–44, –60, –4
	Left Lingual Gyrus	40	–14, –76, –16
	Right Cingulate Gyrus	39	12, 24, 36
MOTO	Left Inferior Parietal Lobule	41	–44, –42, 42
	Right Insula	26	42, 6, 20

We constructed activation maps for seven independent brain networks in 3 year olds and 5 year olds in the resting state. These included the dorsal attention network (DAN), the salience network (SN), the default mode network (DMN), the left frontoparietal network (LFP), the right frontoparietal network (RFP), the executive control network (ECN), and the motor network (MOTO). *X*, *Y*, *Z*: Coordinates are shown in Montreal Neurological Institute (MNI) space for the peak voxel in each activated region. Vol: The voxel size is 3 mm × 3 mm × 3 mm. $P = 0.01$, $t(14) = 2.977$.

frontal gyrus were activated; we did not find activation in the frontal gyrus or temporal gyrus. This indicates that the brain nodes in the children were immature. We found that a PCC-MeFG network connection had formed in the 3-year-old children, while an IPL-MeFG network connection had formed in the 5-year-old children. Additionally, high-correlation connections were strengthened in the 5-year-old children. Specifically, the regional network connections between the left and right hemispheres were significantly enhanced compared with the 3-year-old children, and we found particularly high-correlation network connections in the frontal gyrus. The IPL was the central region in the DMN. However, this network connection was immature in both the 3- and 5-year-old children.

Dorsal attention network: The parietal and frontal networks had formed but were incomplete in the 3-year-old group. We found that more activation nodes had formed in the 5-year-old group compared with the 3-year-old group, suggesting that this network develops rapidly during this period. The high-correlation network connections in 3 and 5-year-olds are a feature of "connection generalization". Generalized network connections decrease and become more specialized with age, and high-efficiency network connections increase, as indicated by the "efficiency and savings" principle.

Executive control network: In the two groups of children, this network activated the left and right IFG. The parietal lobule and temporal gyrus appeared to be undergoing unstable development in both the 3- and 5-year-old children, and nodes were sparse, which may be related to deficiencies in self-control observed in early childhood. High-correlation network connections included the frontal network, the temporal-parietal network, the PCC network, the IPL, and the MeFG, all of which are central nodes. In the 3-year-old children, only the parietal lobule high-correlation network had formed, while higher-correlation network connections such as the frontal network and temporal-parietal network had emerged in the 5-year-old children, indicating rapid development at this age. The executive control network was not mature in the 3- or 5-year-old children.

Executive function may work to activate more frequently-occurring brain configurations while simultaneously avoiding less frequent brain configurations associated with low-vigilance states.

Left frontoparietal network: The network nodes include the frontal gyrus, temporal gyrus, parietal lobule, and cingulate gyrus. The parietal lobule, frontal gyrus, and temporal gyrus nodes had formed in both the 3 and 5-year-olds.

The high-correlation network connections included the frontoparietal network, left-right frontal network, left-right parietal network, and left-right temporal network. High-correlation connections in the frontoparietal network had formed in the 3- and 5-year-old groups, but the high-correlation connections in the left-right network had not formed. Thus, frontoparietal network development does not simply increase with age but appears to change dynamically. High-correlation connections that appeared in the 3-year-old group might have been replaced with new high-correlation connections in the 5-year-old group, *via* a "trade-off". The IPL was the central node in all two groups.

Right frontal parietal network: In this network, the main nodes were the frontal gyrus, parietal lobule, and temporal gyrus, which were activated in the two groups. The central node was not clear in the groups of children.

The high-correlation network was mainly limited to the left-right parietal lobule and the left-right temporal gyrus, and frontoparietal high-correlation network connections had not yet formed in the 3-year-old group. The frontal and left-right MTG connections were strengthened in the 5-year-old group compared with the 3-year-old group, but the IPL central node had not yet formed. The number of high-correlation edges in the 5-year-old group exceeded that of the 3-year-old group.

Salience network: The representative brain areas of the salience network included the inferior frontal gyrus, anterior insula, anterior cingulate, and cingulate gyrus. These brain areas were activated in both the 3- and 5-year-olds. The nodes and network connections with high correlations were generalized in the 3-year-old group, indicating that specialization had yet to occur.

Discussion

Default mode network

Our study design differed from those of previous studies.

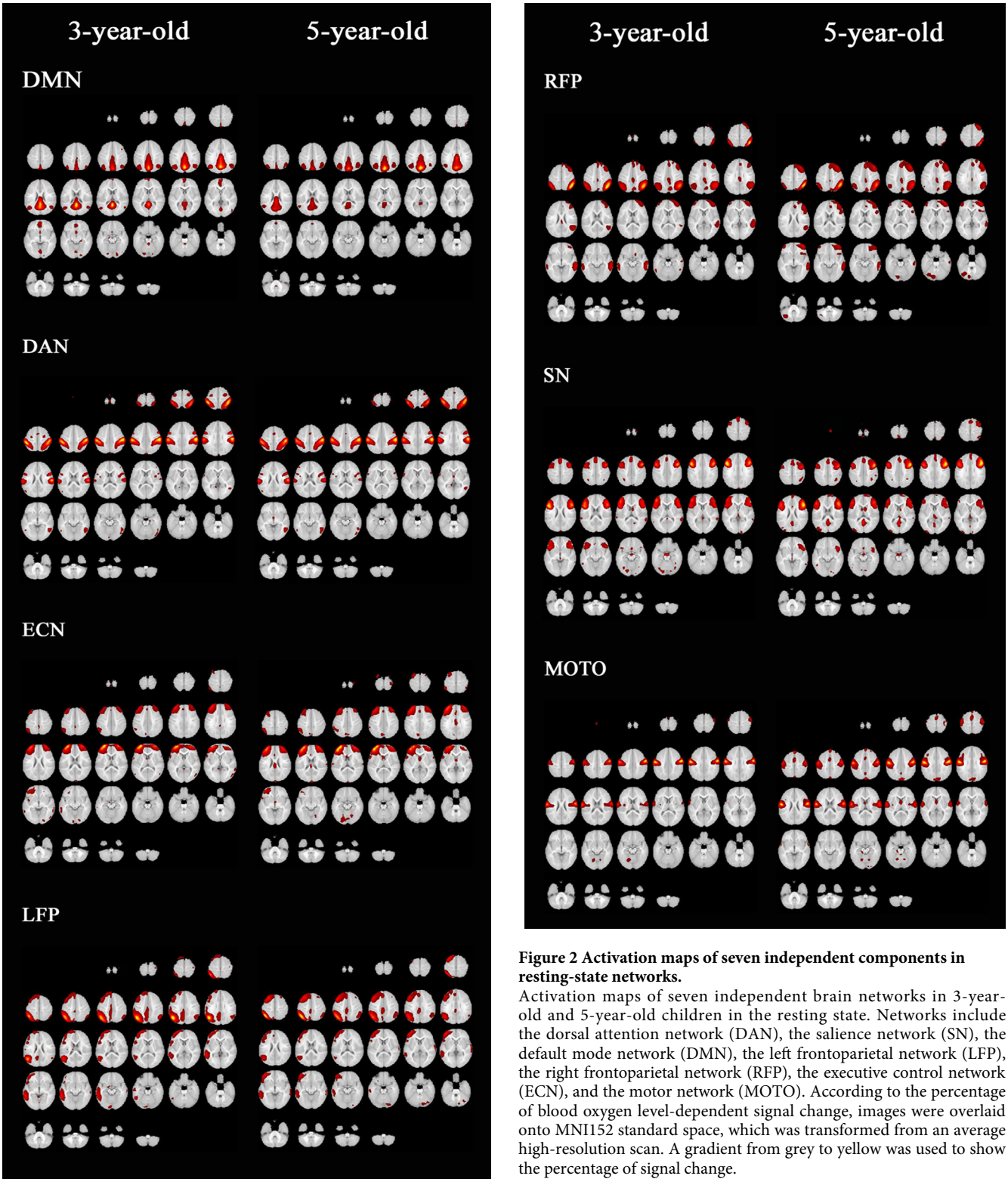

Figure 2 Activation maps of seven independent components in resting-state networks.
Activation maps of seven independent brain networks in 3-year-old and 5-year-old children in the resting state. Networks include the dorsal attention network (DAN), the salience network (SN), the default mode network (DMN), the left frontoparietal network (LFP), the right frontoparietal network (RFP), the executive control network (ECN), and the motor network (MOTO). According to the percentage of blood oxygen level-dependent signal change, images were overlaid onto MNI152 standard space, which was transformed from an average high-resolution scan. A gradient from grey to yellow was used to show the percentage of signal change.

Previous statistical analyses have mainly focused on the differences between two groups, using statistical methods such as regression analysis, difference examination (Wang et al., 2017), related statistics, and activation intensity (Jiang et al., 2018; Margolis et al., 2018). To our knowledge, this study was the first to use network core components (node, edge, core) to analyze brain development in pre-school aged children. We mainly focused on the core brain regions in the network, and the determination of brain regions that were highly correlated with the core brain areas. Previous studies have mainly focused on changes in activation intensity that accompany aging. First, we found that as age increased, brain activation in

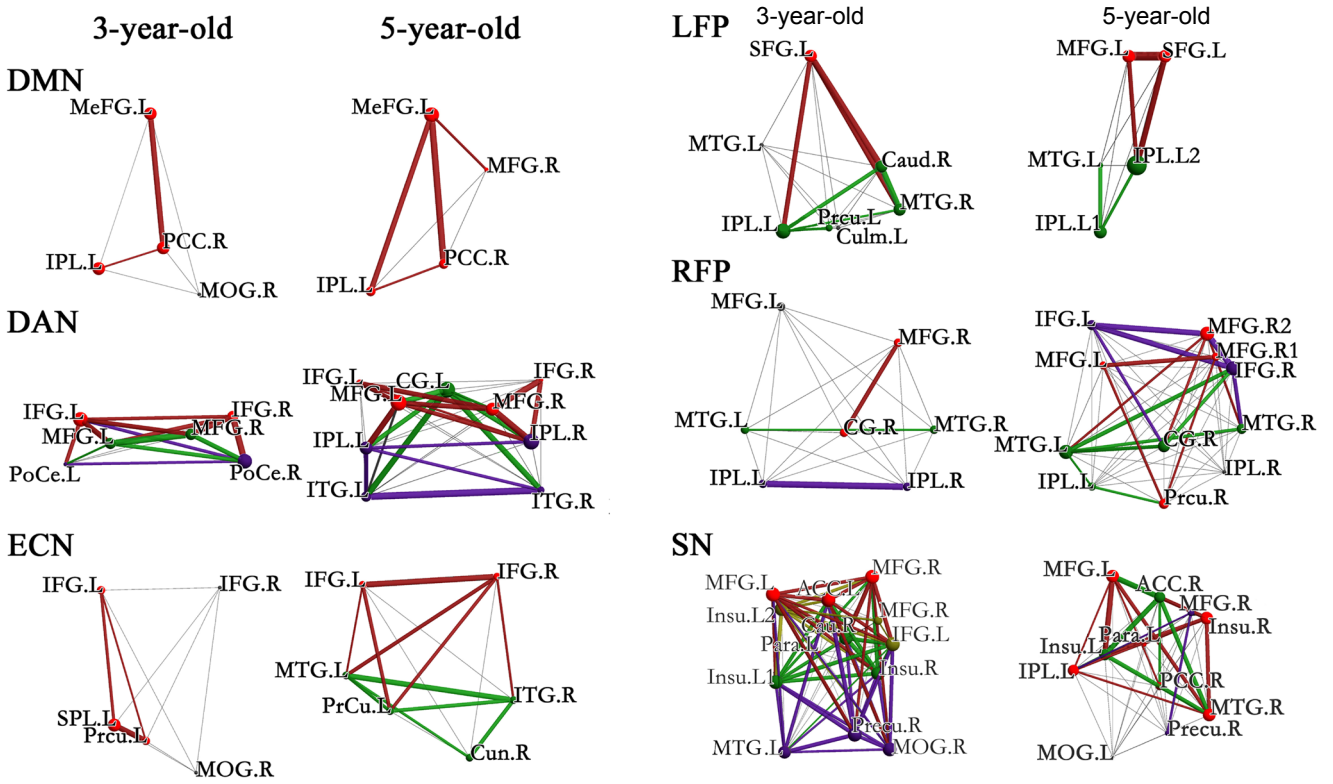

Figure 3 Functional network connectivity in healthy children in the resting state *via* independent component analysis and the BrainNet Viewer.
The correlation network matrix including the dorsal attention network (DAN), the salience network (SN), the default mode network (DMN), the left frontoparietal network (LFP), the right frontoparietal network (RFP), the executive control network (ECN), and the motor network (MOTO) was visualized using the BrainNet Viewer (Xia et al., 2013; http://www.nitrc.org/projects/bnv). The parameters were set as follows: surface opacity = 0, node size value = auto, scale = 0.7, edge threshold = 0.60 (edges larger than 0.60 are displayed as a bold line). The colored lines represent the connectivity strength of different functional networks, as in Figure 3. Abbreviations as shown in Table 1.

connected brain regions increased, but the intensity of the activation weakened and the strength of connections decreased. This decrease may mark the beginning of brain specialization. Our analysis of each component is as follows.

Our principal findings were related to the default-network structure and its functional connections. First, in terms of network node development, the posterior cingulate, inferior parietal lobule, and medial frontal gyrus were activated in both 3- and 5-year-olds. As previously reported, the core brain areas utilized in the adult default mode are the PCC/Rsp, bilateral IPLs, and medial prefrontal cortex (Raichle et al., 2001; Fox et al., 2005; Buckner et al., 2008), and the medial temporal lobe is sometimes active (Buckner et al., 2008). In addition, the default network has specialized subsystems that converge on two main "hubs," specifically, the PCC/Rsp and medial prefrontal cortex. This signifies functional differentiation in the default network (Gao et al., 2009).

In one study, the default mode network was roughly divided into three major sections: the dorsal medial prefrontal cortex; the ventral medial prefrontal cortex; and the region containing the PCC, adjacent precuneus, and lateral parietal cortex (Raichle, 2015).

First, we identified the PCC, IPL, and MeFG as the three basic nodes of the default network in young children. However, our findings are inconsistent with a previous default network study that showed that default networks in children were similar to those in adults, including activation of the lateral temporal cortex (Gao et al., 2009).

Second, in terms of functional connectivity networks, the PCC, IPL, and MePG nodes were highly correlated. We verified that the PCC/Rsp and medial prefrontal cortex were the two main "hubs" of the default network in the resting state networks of children.

Third, in terms of functional connectivity network development in 3- and 5-year-old children, we found a high correlation between MeFG.L and PCC.R in the 3-year-old group and between MeFG and IPL.L in the 5-year-old group.

Consistent with our findings, previous studies have indicated that the functional connections between the medial prefrontal cortex (ventral) and lateral parietal regions/posterior cingulate are stronger in adults than in children aged 7 to 9 (Fair et al., 2008). In general, however, the network in 7 to 9 years old was only sparsely connected. As shown in **Figure 3**, we did not find any single orphan junctions between two nodes, but rather multilateral connections such that one node was connected to multiple nodes. This indicates that the network has already formed in 3- and 5-year-old children.

In 7 to 9 years old, no network is present but sparse connections exist, suggesting that the seed regions for the adult default/task-negative network were employed (Fair et al., 2008). An ICA comparison indicated that the seed correlation is susceptible to human factors. There is no evidence

that the seed coordinates of default networks are the same in adults and children. In our masked ICA data, we specified a distance threshold of 0.7, and found that highly correlated activated areas were clustered in one component. Correlation tests performed in these regions clearly revealed the representative nodes and network connections.

The PCC.R, MeFG, and IPL.L were central nodes in the two groups, which was consistent with a study of 1- and 2-year-old children (Gao et al. 2009).

As shown in **Table 1**, the temporal gyrus was not activated in the 3- or 5-year-old group. Both one-sample and two-sample t-tests indicated that the temporal gyrus develops with age. This may explain why the medial temporal lobe is sometimes involved in part of the default mode network (Buckner et al., 2008). The developing regions were mainly located in the IPL and posterior cingulate, which indicates that the main brain areas of the default mode network had not matured in 3- or 5-year old children.

In individuals with autism, resting state networks are characterized by decreased functional connectivity in the default mode network and executive network (Bi et al., 2018). This is in strong contrast with the size of the brain activation area and high-correlation connections in neurotypical children.

Dorsal attention network development

Table 1 shows our ICA and one-sample *t*-test results for anatomical node development. We found that only the frontal nodes were activated in 3-year-old children; with no activation of the parietal lobule or temporal nodes. The parietal lobule and temporal nodes were clearly activated in the 5-year-old group, as were the parietal lobule and temporal gyrus. These findings are somewhat consistent with those of a study of 4- to 9-month-old children (Damaraju et al., 2014). However, in that study, the researchers observed activation in the right IFG (BA 44) and left IFG (BA 45) only; while the IPL was not activated. However, they did find that activation of the frontal lobule first appeared in early childhood, which is consistent with our findings.

In terms of functional connection network development, we observed certain significant correlations with respect to the dorsal attention network: (1) A number of high correlation edges were present in the 3- and 5-year-old groups. In the 3-year-old group, connections between the frontal lobule, parietal connection, and temporal connection did not appear. In the 5-year-old group, there were strong correlations between the IPL.L-IPL.R, ITG.L-ITG.R, and IFG.L-MFG.R, etc. (2) The connection between the left and right hemispheres was clearly strengthened in 5-year-olds compared with 3-year-olds. (3) In both groups, the number of high correlation edges was greater than that observed in adults, indicating that dorsal attention network specialization had yet to occur such that the connections were instead generalized.

A previous study described two neural systems for stimulus-driven attention and goal-directed states within the adult human brain: the dorsal attention network, centered in the intraparietal sulcus and frontal eye fields, and the ventral attention network, anchored in the ventral frontal cortex and temporoparietal junction (Farrant and Uddin, 2015).

Compared with stimulus-driven attention and goal-directed states, the resting state in adults is characterized by a lack of cognitive processing associated with stimuli and targets as well as decreased activation of the frontal cortex compared with the intraparietal cortex. The intraparietal cortex is the only core node, as seen in **Figure 2** (ICA picture) and Figure 3 (connection network). Finally, the temporoparietal cortex and inferior frontal cortex are primarily lateralized to the right hemisphere (e.g., Corbetta and Shulman, 2002).

Resting-state network connections in children have the following features: (1) functional connectivity within regions is greater in children, as found in a resting-state network study of 7- to 12-year-old children (Farrant and Uddin, 2015); and (2) the connection between the left and right hemispheres is strengthened rather than lateralized to the right hemisphere.

In the dorsal attention network, the main brain areas that differed between the 5-year-olds and 3-year-olds were the frontal gyrus and parietal lobule, revealing that these are the main brain areas that undergo development from ages 3 to 5. The dorsal attention network consists of the intraparietal sulcus/superior parietal lobe and the frontal eye fields (Dosenbach et al., 2007). The development of the attention network occurs mainly in the dorsal attention network.

In terms of connections in the resting ICA network, functional connectivity in this network is altered in individuals with Autism Spectrum Disorder, with particular increases in the dorsal attention network (Bi et al., 2018; Rohr et al., 2018).

Information regarding each brain functional network is given in **Additional file 3**.

Conclusions

Our data indicate that the motor network is similar in preschool children aged 3 and 5 years, while other networks appeared to develop between these two time points. In particular, compared with adults, the nodes in children's brains are less developed, and existing network connections are not specialized. Three types of development appear to occur: first, the brain network grows with age; for example, of the basic nodes involved in the default mode network, only the inferior parietal lobule, PCC, and the medial frontal gyrus appear in 3- and 5-year-old children. Second, dynamic changes, or trade-offs, occur. Relatively strong nodes or connections that appear in younger children appear to weaken or disappear with age, and new nodes or connections may appear. Many network connections were strong in the 3- and 5-year-old children; for example, in the dorsal attention network, high correlation connections were present in the IPL.L-IPL.R and ITG.L-ITG.R networks of 5-year-olds. Third, in the children in the present study, some networks were generalized, and specialized networks had not formed. For example, in the salience network, the number of network nodes and high-correlation connections in 3-year-old children exceeded that found in 5-year-old children, while in the dorsal attention network, we found highly correlated network connections in both the 3- and 5-year-old children.

Author contributions: *Implementation of the experiments, data acquisition, data analysis, manuscript preparation and manuscript editing: CLL and YJD; data analysis and acquisition: YHH; study concept and manuscript editing: HCZ; and study concept and study design: CLL; manuscript preparation and editting: FCJ. All authors approved the final version of the paper.*
Conflicts of interest: *The authors have no conflicts of interest to declare.*
Financial support: *This work was supported by the Natural Science Foundation of Guangdong Province, No. 2016A030313180 (to FCJ). The funding body played no role in the study design, in the collection, analysis and interpretation of data, in the writing of the paper, and in the decision to submit the paper for publication.*
Institutional review board statement: *The procedures followed were approved by the Academic Ethics Committee of Shenzhen Institutes of Advanced Technology, Chinese Academy of Sciences (approval No. SIAT-IRB-131115-H0075) on November 15, 2013. The study protocol conformed to the ethical guidelines of the 1975 Declaration of Helsinki as reflected in a prior approval by the institution's human research committee.*
Declaration of patient consent: *The authors certify that they have obtained all appropriate participants' consent forms from their parents. In the forms the participants' parents have given the consent for participants' images and other clinical information to be reported in the journal. The participants' parents understand that participants' names and initials will not be published and due efforts will be made to conceal their identity.*
Reporting statement: *This study followed the Strengthening the Reporting of Observational Studies in Epidemiology (STROBE) statement.*
Biostatistics statement: *The statistical methods of this study were reviewed by the biostatistician of South China Normal University, China.*

Data sharing statement: *Individual participant data that underlie the results reported in this article, after deidentification (text, tables, figures, and appendices) will be in particular shared. Study protocol form will be available. The data will be available immediately following publication without end date. Anonymized trial data will be available indefinitely at www.figshare.com.*
Plagiarism check: *Checked twice by iThenticate.*
Peer review: *Externally peer reviewed.*

Open peer reviewer: *Gregory Wohl Kirschen, Stony Brook University, USA.*
Additional files:
Additional file 1: *Hospital Ethics Approval (Chinese and English).*
Additional file 2: *Informed Consent Documentation (Chinese).*
Additional file 3: *The information on each brain functional network.*
Additional file 4: *Open peer review report 1.*

References

Bi XA, Zhao J, Xu Q, Sun Q, Wang Z (2018) Abnormal functional connectivity of resting state network detection based on linear ica analysis in autism spectrum disorder. Front Physiol 9:475.
Biswal B, Yetkin FZ, Haughton VM, Hyde JS (1995) Functional connectivity in the motor cortex of resting human brain using echo-planar MRI. Magn Reson Med 34:537-541.
Buckner RL, Andrews-Hanna JR, Schacter DL (2008) The brain's default network: anatomy, function, and relevance to disease. Ann N Y Acad Sci U S A 1124:1-38.
Corbetta M, Shulman GL (2002) Control of goal-directed and stimulus-driven attention in the brain. Nat Rev Neurosci 3:201-215.
Cox RW (2012) AFNI: what a long strange trip it's been. Neuroimage 62:743-747.
Damaraju E, Caprihan A, Lowe JR, Allen EA, Calhoun VD, Phillips JP (2014) Functional connectivity in the developing brain: a longitudinal study from 4 to 9 months of age. Neuroimage 84:169-180.
de Bie HM, Boersma M, Adriaanse S, Veltman DJ, Wink AM, Roosendaal SD, Barkhof F, Stam CJ, Oostrom KJ, Delemarre-van de Waal HA, Sanz-Arigita EJ (2012) Resting-state networks in awake five- to eight-year old children. Hum Brain Mapp 33:1189-1201.
Deng Z, Chandrasekaran B, Wang S, Wong PC (2016) Resting-state low-frequency fluctuations reflect individual differences in spoken language learning. Cortex 76:63-78.
Doria V, Beckmann CF, Arichi T, Merchant N, Groppo M, Turkheimer FE, Counsell SJ, Murgasova M, Aljabar p, Nunes RG, Larkman DJ, Rees G, Edwards AD (2010) Emergence of resting state networks in the preterm human brain. Proc Natl Acad Sci U S A 107:20015-20020.
Dosenbach NU, Fair DA, Miezin FM, Cohen AL, Wenger KK, Dosenbach RA, Fox MD, Snyder AZ, Vincent JL, Raichle ME, Schlaggar BL, Petersen SE (2007) Distinct brain networks for adaptive and stable task control in humans. Proc Natl Acad Sci U S A 104:11073-11078.
Fair DA, Cohen AL, Dosenbach NU, Church JA, Miezin FM, Barch DM, Raichle ME, Petersen SE, Schlaggar BL (2008) The maturing architecture of the brain's default network. Proc Natl Acad Sci U S A 105:4028-4032.
Farrant K, Uddin LQ (2015) Asymmetric development of dorsal and ventral attention networks in the human brain. Dev Cogn Neurosci 12:165-174.
Fox MD, Snyder AZ, Vincent JL, Corbetta M, Van Essen DC, Raichle ME (2005) The human brain is intrinsically organized into dynamic, anticorrelated functional networks. Proc Natl Acad Sci U S A 102:9673-9678.
Gao W, Zhu H, Giovanello KS, Smith JK, Shen D, Gilmore JH, Lin W (2009) Evidence on the emergence of the brain's default network from 2-week-old to 2-year-old healthy pediatric subjects. Proc Natl Acad Sci U S A 106:6790-6795.
Gomot M, Bernard FA, Davis MH, Belmonte MK, Ashwin C, Bullmore ET, Baron-Cohen S (2006) Change detection in children with autism: an auditory event-related fMRI study. NeuroImage 29:475-484.
Grossmann T, Striano T, Friederici AD (2007) Developmental changes in infants' processing of happy and angry facial expressions: a neurobehavioral study. Brain Cogn 64:30-41.
Jafri MJ, Pearlson GD, Stevens M, Calhoun VD (2008) A method for functional network connectivity among spatially independent resting-state components in schizophrenia. Neuroimage 39:1666-1681.
Jiang P, Vuontela V, Tokariev M, Lin H, Aronen ET, Ma Y, Carlson S (2018) Functional connectivity of intrinsic cognitive networks during resting state and task performance in preadolescent children. PLoS One 13:e0205690.
Konishi Y, Taga G, Yamada H, Hirasawa K (2002) Functional brain imaging using fMRI and optical topography in infancy. Sleep Med 3:S41-S43.
Lee MH, Smyser CD, Shimony JS (2013) Resting-state fMRI: a review of methods and clinical applications. AJNR Am J Neuroradiol 34:1866-1872.
Lenneberg EH (1967) Biological Foundation of Language. New York: Wiley, USA.
Lin W, Wu H, Liu Y, Lv D, Yang L (2017) A CCA and ICA-based mixture model for identifying major depression disorder. IEEE Trans Med Imaging 36:745-756.
Margolis AE, Pagliaccio D, Thomas L, Banker S, Marsh R (2018) Salience network connectivity and social processing in children with nonverbal learning disability or autism spectrum disorder. Neuropsychology doi: 10.1037/neu0000494.
Moher Alsady T, Blessing EM, Beissner F (2016) MICA-A toolbox for masked independent component analysis of fMRI data. Hum Brain Mapp 37:3544-3556.
Mostert JC, Shumskaya E, Mennes M, Onnink AM, Hoogman M, Kan CC, Arias Vasquez A, Buitelaar J, Franke B, Norris DG (2016) Characterising resting-state functional connectivity in a large sample of adults with ADHD. Prog Neuropsychopharmacol Biol Psychiatry 67: 82-91.
Muetzel RL, Blanken LM, Thijssen S, van der Lugt A, Jaddoe VW, Verhulst FC, Tiemeier H, White T (2016) Resting-state networks in 6-to-10 year old children. Hum Brain Mapp 37:4286-4300.
Nomi JS, Uddin LQ (2015) Developmental changes in large-scale network connectivity in autism. Neuroimage Clin 7:732-741.
Penfield W, Roberts L (1959) Speech and Brain Mechanisms. New Jersey: Princeton University Press, USA.
Raichle ME (2015) The brain's default mode network. Annu Rev Neurosci 38:433-447.
Raichle ME, MacLeod AM, Snyder AZ, Powers WJ, Gusnard DA, Shulman GL (2001) A default mode of brain function. Proc Natl Acad Sci U S A 98:676-682.
Rohr CS, Arora A, Cho IYK, Katlariwala P, Dimond D, Dewey D, Bray S (2018) Functional network integration and attention skills in young children. Dev Cogn Neurosci 30:200-211.
Thomason ME, Dennis EL, Joshi AA, Joshi SH, Dinov ID, Chang C, Henry ML, Johnson RF, Thompson PM, Toga AW, Glover GH, Van Horn JD, Gotlib IH (2011) Resting-state fMRI can reliably map neural networks in children. Neuroimage 55:165-175.
Wang Y, Li Y, Wang H, Chen Y, Huang W (2017) Altered default mode network on resting-state fmri in children with infantile spasms. Front Neurol 8:209.
Xia M, Wang J, He Y (2013) BrainNet Viewer: a network visualization tool for human brain connectomics. PLoS One 8:e68910.
Xiao Y, Zhai H, Friederici AD, Jia F (2016) The development of the intrinsic functional connectivity of default network subsystems from age 3 to 5. Brain Imaging Behav 10:50-59.
Zhang H, Zuo XN, Ma SY, Zang YF, Milham MP, Zhu CZ (2010) Subject order-independent group ICA (SOI-GICA) for functional MRI data analysis. Neuroimage 51:1414-1424.

P-Reviewer: Kirschen GW; C-Editor: Zhao M; S-Editors: Wang J, Li CH; L-Editors: Koke S, Wang L, Song LP; T-Editor: Liu XL